Geoderma 363 (2020) 114154

Contents lists available at ScienceDirect

Geoderma

journal homepage: www.elsevier.com/locate/geoderma

Impact of potential bio-subsoilers on pore network of a severely compacted subsoil

Mansonia Pulido-Moncada[a,*], Sheela Katuwal[a], Lidong Ren[b], Wim Cornelis[b], Lars Munkholm[a]

[a] Aarhus University, Department of Agroecology, Research Centre Foulum, Blichers Allé 20, P.O. Box 50, DK, 8830 Tjele, Denmark
[b] Ghent University, Department of Environment, Coupure Links 653, 9000 Ghent, Belgium

ARTICLE INFO

Keywords:
Lucerne (alfalfa)
Chicory
X-ray Computed Tomography
Pore network

ABSTRACT

Subsoil compaction is a major threat to soil quality. The use of bio-subsoilers has been proposed as a mitigation practice. There is, however, a paucity of knowledge on the effects of potential bio-subsoiling crops in alleviating severely compacted subsoil. X-ray Computed Tomography (CT) was used to assess the changes caused by different crops in the pore network of a severely compacted subsoil. The potential bio-subsoilers, chicory, lucerne, radish and tall fescue, with spring barley as reference, were grown for one year in undisturbed soil columns (Ø = 0.20 m, h = 0.50 m) with soil originating from a heavily compacted soil after mechanical impact. Soil columns were X-ray CT-scanned before and after the experiment. CT-pore soil characteristics were quantified by image analysis. Crop treatments affected the soil porosity differently on the studied soil. Radish and tall fescue did not show a significant impact on CT-derived pore characteristics at any depth. In the compacted layer, the macropore density, the branches number, and the number of pores (for volume sizes of < 100 mm^3 and diameter ≤ 1.5 mm) were larger for chicory and lucerne compared to barley ($P < 0.05$). Chicory and Lucerne appear to contribute to the development of a large number of complex-shaped pores. Differences in the CT-derived pore network indicate that chicory and lucerne are likely to perform better than the other crops when used as bio-subsoilers by creating a larger, more connected and complex pore network. Longer-term growth is needed to obtain a marked loosening effect in the compacted layer.

1. Introduction

Soil compaction due to heavy vehicular traffic in wet conditions is one of the degradation problems in agricultural soils that severely affects crop growth due to its adverse effects on soil structure-related properties (Arvidsson, 2001; Lipiec and Hatano, 2003; Arvidsson and Håkansson, 2014). Soil compaction reduces pore volume, and causes disruption of pore characteristics that affects water and gas flow, as well as increases soil density and soil penetration resistance, which together contribute to a reduction on plant rootability, among others effects (Materechera et al., 1991). The effects of soil compaction on soil characteristics have been found to be persistent, especially in the subsoil below tillage depth (Berisso et al., 2013; Etana et al., 2013).

Subsoil compaction, therefore, is a severe problem because it hampers agricultural production and impacts the environment (Jones et al., 2003), but also because its natural recovery rate is slow (Munkholm et al., 2005).

Subsoil compaction mitigation can be initiated by anthropogenic mechanisms (e.g., mechanical loosening), as well as natural mechanisms that involves abiotic (e.g., wetting–drying and freezing-thawing) or biotic (e.g., plant roots and earthworm activities) processes (Keller et al., 2017).

A challenge for biotic mechanisms in the soil structure recovery lies on the fact that the poor soil physical conditions prevailing in compacted subsoil layers limit root development (Materechera et al., 1991). However, crop response depends on differences between species in the ability of roots to overcome soil compaction or physical impedance by different mechanisms, e.g. growth pressure, elongation rate, thickness or diameter, radial swelling, root anchorage (Löfkvist, 2005; Lynch and Wojciechowski, 2015).

Deep-rooted crops with the potential to penetrate hard layers have been assessed and proposed as bio-subsoilers (Cresswell and Kirkegaard, 1995; Löfkvist, 2005; Chen and Weil, 2010). The term bio-subsoilers here, refers to plants with root systems that have the potential to penetrate compacted soil layers and act as biotic mechanisms for soil compaction mitigation.

The changes in soil structure brought about by bio-subsoilers, commonly used as cover crops, are linked to the creation of fissures and

* Corresponding author.
E-mail address: mansonia.pulido@agro.au.dk (M. Pulido-Moncada).

https://doi.org/10.1016/j.geoderma.2019.114154
Received 26 July 2019; Received in revised form 18 December 2019; Accepted 20 December 2019

biopores that can improve water movement and gas flow through the dense layers (Materechera et al., 1992), and these biopores can also be reused by subsequent crop roots (Chen and Weil, 2011). The reuse of biopores allows roots to explore the compacted layer for nutrients and water (Cresswell and Kirkegaard, 1995).

The potential of plant species to be used for compaction mitigation has been found to differ between monocotyledons (fibrous-rooted) and dicotyledons (tap-rooted) (Clark and Barraclough, 1999; Chen and Weil, 2010). The pattern of root growth of monocotyledonous plants, such as grasses, consists of seminal and adventitious roots growing from the basal nodes of the shoot with approximately uniform size along their length. In contrast, the dicotyledonous root system (e.g., brassicas) is characterised by a vertical growing taproot, derived from the radicle, and lateral roots of smaller diameter, with the taproot creating continuous biopores to deep layers (Löfkvist, 2005).

The most common cover crops that have been assessed as potential bio-subsoilers are fodder radish (*Raphanus sativus* L.), lucerne (alfalfa) (*Medicago sativa* L.), tall fescue (*Festuca arundinacea* L.), rapeseed (*Brassica napus*, cultivar 'Essex'), rye (*Secale cereale* L.), canola (*Brassica rapa* L.) and English ryegrass (*Lolium perenne* L.) (Raper et al., 2000; Williams and Weil, 2004; Weil and Kremen, 2007; Celette et al., 2008; Chen et al., 2014). These cover crops were found to decrease bulk density and penetration resistance and increase porosity, hydraulic conductivity, soil moisture and water-holding capacity down to 0.60 m depth (Materechera et al., 1992; Löfkvist, 2005; Hubbard et al., 2013). However, the limited profitability, high cost of establishment, diseases and weed problems are some of the concerns associated with the above-mentioned cover crops (Snapp et al., 2005).

The benefits from the use of bio-subsoilers for root growth, water and nutrient uptake, and yield of subsequent crops are expected to be time-, site- and crop type-dependent. Consequently, the changes induced by the bio-subsoilers to the standard soil physical parameters that are used as indicators for soil structure could be negligible at initial stages of soil compaction mitigation. Therefore, the most sensible approach to evaluating the existence of soil structural changes caused by root channels and any other type of biopores is the characterisation of the pore network (Cresswell and Kirkegaard, 1995) and for this there is only limited information available on the effects of root development on soil pore characteristics in heavily compacted subsoil layers.

The non-destructive imaging techniques such as X-ray Computed Tomography (CT) allows visualisation of the spatial distribution of soil pores and the quantification of changes in pore characteristics (Głąb, 2007; Luo et al., 2010). Therefore, the 3D geometrical characterisation of the soil pore network provides a better understanding of soil pore measurements and their relation with soil hydraulic functions, solute transport, preferential flow, water-soil-root interaction, and management practices (e.g., Carminati et al., 2009; Naveed et al., 2013; Katuwal et al., 2015c). Previous studies have used 3D image analysis techniques to evaluate the impact of soil compaction on soil functions (e.g., Lamandé et al., 2013; Naveed et al., 2016) and root system architecture (e.g., Zappala et al., 2013; Pfeifer et al., 2015). However, studies evaluating the effect of different plant species on soil compaction mitigation revealed by X-ray CT of large column samples are scarce.

This study evaluated the changes caused by different bio-subsoilers in the pore network of a severely compacted subsoil located in a humid northern European agricultural area. Geometrical soil pore characteristics were assessed and quantified at three different soil depths using a medical X-ray CT scanner. It was hypothesised that the selected crops, as bio-subsoilers, would affect soil pore network positively and differently by penetrating and loosening the severely compacted soil.

2. Materials and methods

2.1. Soil samples

Samples were taken from a sandy loam soil located at Aarslev site in Denmark (55°18′18″N, 10°26′52″E). Previous to the sampling, a compaction experiment with farm machinery traffic had been conducted over four consecutive years (2010–2013). A detailed description of this compaction experiment can be found in Schjønning et al. (2016). In the present study, the soil samples were taken from the treatment that caused the most severe compaction after traffic stress, labelled M8 (78 kN) in previous publications (Schjønning et al., 2016; Pulido-Moncada et al., 2019). Briefly, the M8 compaction treatment involved multiple passes (4–5) of a tractor and slurry trailer combination applying an 8 Mg wheel load on the middle and rear trailer axles. The tyre inflation pressure of the tractor was 150–300 kPa, and the mean ground pressure was 56–161 kPa.

The experimental traffic under the M8 treatment resulted in a high degree of compaction (101%) at 0.30 m depth, characterised by a high bulk density (1.77 Mg m^{-3}) and a reduction in pore volume (air-filled porosity of 0.08 m^3 m^{-3}) and gas flow (air permeability of 2.3 μm^2) as compared to the non-trafficked control (Pulido-Moncada et al., 2019).

More specifically, in the M8 plot that was selected for sampling in the present study, the soil was characterised by 4, 26, 70 and 0.23 g 100 g^{-1} of clay (< 2 μm), silt (2–63 μm), sand (63–2000 μm) and soil organic carbon content, respectively, a bulk density of 1.72 Mg m^{-3} and a total pore volume of 0.35 m^3 m^{-3} at 0.30 m depth (data taken from block 1 of the dataset analysed by Pulido-Moncada et al. (2019)).

From the selected M8 plot, soil samples (Ø = 0.20 m, h = 0.50 m) were randomly extracted in spring 2017 by driving aluminium cores vertically into the soil with the hydraulic press of a tractor. The soil samples were manually excavated and transported to the Foulum site (56°29′06.5″N, 9°34′56.7″E), in Denmark.

2.2. Experimental treatments

In this study, fifteen soil samples were X-ray CT-scanned immediately after sampling. Afterwards, an experimental plot (about 24 m^2) for installing the soil cores was prepared at the Foulum site by excavating the top 0.50 m soil in an area with a homogeneous subsoil layer in terms of texture (10.6, 26.0 and 63.4 g 100 g^{-1} of clay, silt and sand, respectively) and bulk density (average of 1.90 Mg m^{-3}). All the soil cores were placed vertically in the experimental plot with the bottom in contact with the subsoil at 0.50 m depth, the top level with the soil surface and with the space between the soil columns refilled with the excavated soil (Fig. 1).

The experiment was established with treatments consisting of spring barley (*Hordeum vulgare* L.) as the reference and four potential bio-subsoilers, i.e., chicory (*Cichorium intybus*), lucerne (*Medicago sativa* L.), fodder radish (*Raphanus sativus* L.) and tall fescue (*Festuca arundinacea* L.), in three replicates, using a complete randomised design. The reference used in our research counts for the root system of spring barley in interaction with bioturbation and dry/wet cycles happening in the soil under study. Bioturbation and weathering was however a common factor in our control as in the plant treatments.

Seeding in the soil cores was conducted in May 2017 with a seeding rate of 150, 3, 25, 10 and 12 kg ha^{-1} for spring barley, chicory, lucerne, radish and tall fescue, respectively, following the common agricultural practice in Denmark. Fertilisation took place after germination in June 2017 and in May 2018 with 140 kg N ha^{-1}. The above-ground biomass of all the plants was cut on 26 July 2017. The perennial species were additionally cut successively on 9 September and 17 October 2017. Radish was reseeded in August 2017, hence two growing periods of radish per year. Two times fodder radish was chosen to obtain maximal fodder radish effect on soil structure. In April 2018, spring barley and radish were sown for the second year.

Fig. 1. Installation of the soil samples collected from the Aarslev site at the experimental plot at the Foulum site with the bottom of the samples in contact with the subsoil at 0.50 m depth, and the top level with the soil surface. Samples were installed vertically and surrounded by loose refilled soil.

2.3. Image acquisition and processing

In summer 2018, the 15 previously CT-scanned samples were excavated from the experimental plot, and went under a second scanning event. The soil samples were scanned at field moisture content close to field capacity. For both scanning events, X-ray images were acquired using a medical scanner (Siemens Biograph 64 True Point, Siemens AG, Erlangen, Germany) at the Department of Nuclear Medicine & PET-Centre of Aarhus University Hospital, Aarhus, Denmark. The soil columns were oriented horizontally for each scan. The scanning was performed using a voltage of 140 kV, an exposure time of 1000 ms (exposure of 600 mAs), and an X-ray tube current of 270 mA. The reconstruction was carried out using the manufacturer's software, resulting in a stack of 12-bit images with a slice thickness of 0.6 mm and 512 × 512 pixels per slice. This led to a voxel size of 0.43 × 0.43 × 0.6 mm in the reconstructed image.

The freeware software program ImageJ version 1.52 h (Abràmoff et al., 2004) and the associated plugins were used for image processing and analyses. The procedure of image analyses involved alignment correction, filtering, segmentation, and measurements.

For each image stack, the alignment of the slices was corrected using the 'Untilt Stack' plugin (Cooper, 2011) and the centre of the soil column translated to the centre of the canvas to obtain identical horizontal planes for each column at both scanning events. The aligned images of the 0.50 m of the soil column were cropped to 0.40 m height and to a region of interest (ROI) of 0.16 m diameter to avoid the uneven top soil surface and artefacts near the cylinder wall.

A 3D median filter (radius = 2.0 voxels) and contrast enhancement with saturated pixels of 0.4% were used to reduce the noise in the image and improve the contrast. Image segmentation was conducted by the auto-local threshold algorithm of Phansalkar et al. (2011), with a radius of 7 and default values for other parameters set in ImageJ software (i.e. k = 0.25 and r = 0.5).

In the binary images obtained from segmentation, features made up of 1 voxel were removed to avoid classification of noise in further analysis. Therefore, the pore networks quantified in this study represent macropores equal to or > 0.86 mm in diameter. Macropores with diameter equal to 0.82 mm are truly vertically oriented. The segmented binary images were then visually inspected for artefacts that would result in an overestimation of macroporosity. Artefacts or artificial pores close to the cylinder wall were created during sampling by the displacement of stones. These stone artefacts were manually removed from the binary image by selecting a seed voxel within the artefact and using a region-growing algorithm in the 'MorphoLibJ' plugin (Legland et al., 2016) to obtain all the connected voxels representing the artefact. In instances where the artefact was connected to other visible macropores, erosion and dilation operations were carried out iteratively until the two were disconnected. ImageJ's image calculator tool was used for subtracting the artefacts from the binary images.

All pores developed after 1 year of study, including the biopores created by roots were under consideration. Therefore, the CT-macropores segmented include both macropores and roots. In the chicory treatment, the roots were visible inside the pores (with higher grey level value than pores) and were not segmented as pores by the local thresholding algorithm of Phansalkar et al. (2011). The segmentation of roots for the chicory treatment was achieved by thresholding the roots twice. First, a threshold based on visual inspection was applied and the roots were separated from the noisy segmented image using a region-growing algorithm in the 'MorphoLibJ'plugin (Legland et al., 2016). Then a dilation operation was applied and the foreground voxels were represented by their original grey values. To this image another threshold, which was obtained from the minimum point in the image histogram between the peaks for pores and roots, was applied to segment the roots only. The resulting segmented roots were then added to the segmented pores to obtain the CT-total macropores.

The binary images after correction for holes and including roots in the segmented images were further used for pore quantification and analysis.

2.4. Image analyses

The analyses of the CT-macropores were performed for three layers, i.e. 'Plough', 'Transition' and 'Compacted'. These layers correspond to soil depths of 0.10–0.25, 0.25–0.35 and 0.35–0.50 m. The three soil layers were distinguished based on the compactness of the soil with soil depth, which was assessed using the average grey values of each slice in the ROI. Higher average grey values of slices are associated with more compacted soils in the ROI.

CT-derived pore characterisation analysis (Table 1) was conducted using ImageJ (Abràmoff et al., 2004) and associated plugins. A connected cluster of voxels is considered as a pore in the study. CT-porosity distribution with depth, was achieved by calculating the CT-macroporosity value for each slice of the binary image of each sample. The 'BoneJ' plugin (Doube et al., 2010) was used for quantification of CT-derived macropore characteristics such as pore density, the number of pore clusters per unit volume; genus density or pore connectivity, the number of loops/redundant connection per unit volume (Vogel et al., 2010) and mean pore diameter, the volume-weighted average thickness of pores (Katuwal et al., 2015a) (Table 1).

A skeletonised 3D image for each soil layer was obtained and analysed using the 'Skeletonize' BoneJ-Plugin and the 'Analyse Skeleton' BoneJ-Plugin (Doube et al., 2010). Analyse Skeleton was applied with and without pruning and the results combined to correct the effect of the roughness of the pore walls (Katuwal et al., 2015b). Macropore branch number, total branch length and average tortuosity were derived from the output of the skeletonise 3D image analysis (Table 1).

Additionally, CT-derived pore size and shape distribution were determined for each soil layer. Since the average pore volume or the

Table 1
Description of the soil pore parameters quantified using a medical X-ray Computed Tomography scanner.

Parameter	Calculation	Unit
Macropore density	$\frac{totalnumberofmacropores}{volumeoftheROI}$	Number m^{-3}
Macroporosity	$\frac{totalvolumeofmacropores}{volumeoftheROI}$	$m^3\ m^{-3}$
Macropore area density	$\frac{areaofmacropores}{volumeoftheROI}$	$m^2\ m^{-3}$
Macropore Connectivity or genus density	$\frac{genus}{volumeoftheROI}$ where the genus is the total number of redundant connections or loops in the pore space network contained in a soil column	Number m^{-3}
Mean macropore diameter	$\sum_{i=1}^{n} \frac{d_i V_i}{V_i}$ where d_i and V_i are the diameter and volume of each macropore within the ROI	m
Macropore tortuosity	$\frac{totalmacroporelength}{totalEuclideandistance}$ where the total Euclidean distance is the total shortest distance between the ends of all macropores of the ROI	

ROI is the region of interest

average pore size does not provide information of the variability in the sizes of pores, we compared the effect of different treatments on pore-size distribution using the pore volume intervals representing unit increase in the logarithm (base 10) of pore volume. As the volume distribution of pores is much skewed, we used a logarithmic interval rather than a constant interval. The pores quantified in the manuscript are macropores and roughly > 1 mm, which would be well-drained at field-moisture contents. Various studies (e.g., Luo et al., 2010) have shown that soil pore properties such as pore volumes, lengths, size (diameter), and connectivity are highly correlated, which also implies that large pore volume is associated with higher flow and transport properties than smaller pore volumes. The pore size distribution was determined by CT-total pore volume at five different intervals: < 1; 1–10; 10–100; 100–1000 and > 1000 mm^3, and by pore diameter at five different ranges: < 1.5; 1.5–2.0; 2.0–2.5; 2.5–3.0 and > 3.0 mm. The diameter interval used here denotes an increase per unit voxel width.

For the pore shape classification, the axes indices suggested by Zingg in 1935 and referenced by Bullock et al. (1985) were calculated using the long (L), intermediate (I) and short (S) radius of the best-fit ellipsoid (Fig. 2) obtained from the 'Particle Analyzer' BoneJ plugin (Doube et al., 2010). The axes ratio indices are described in detail in Pires et al. (2019). Large values of I/L and S/I ratios classify pores as spheres and small values as a-circular-planar pores (Fig. 2). The pores were classified as either equant (spherical), oblate (disk-shaped), triaxial (bladed), prolate (rod-like) or non-classified, the last representing pores for which the software could not determine at least one of the axes.

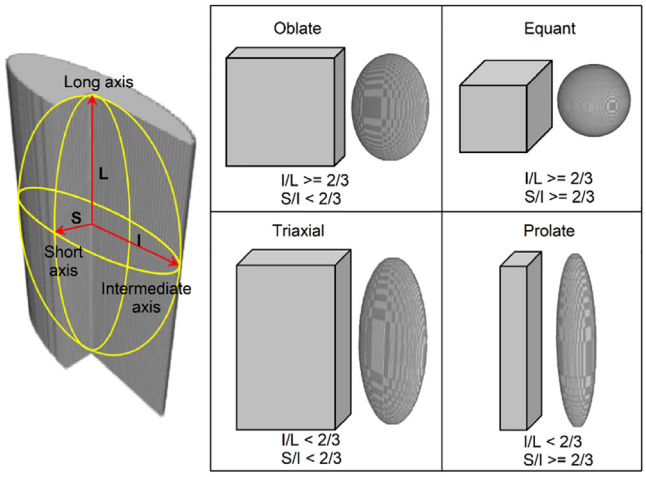

Fig. 2. Illustration of the classification of soil pores based on shapes. The largest ellipsoid that can be fitted within a pore is measured for its diameters along the long axis (L), intermediate axis (I) and short axis (S) (left figure). The ratios between I/L and S/I are used for classifying the pores (right figures). (After Zingg diagram referenced by Bullock, 1985).

2.5. Statistical analyses

The CT-derived pore characteristics were determined by detecting differences between barley (reference) and the potential bio-subsoilers at three different soil depths from 0.1 to 0.5 m. Because pore parameters were not normally distributed, the non-parametric Kruskal-Wallis test was used to test the effect of the plant treatments on the CT-derived pore characteristics, as well as on pore number and pore volume contribution for each size interval of the selected pore distribution. All tests were conducted at 5% significance level. The analyses were performed using the statistical package SPSS (version 24, SPSS Inc., USA).

3. Results

3.1. Pore characteristics

The CT-derived pore characteristics are given in Table 2. Before the establishment of the plant treatments, there was a clear trend of decreasing macropore density with depth, e.g.: 27.4, 3.5 and 0.7 ($\times 10^5$ number m^{-3}) for Plough, Transition and Compacted layer, respectively. The same trend was obtained for CT-macroporosity with average values of 0.0747, 0.0179 and 0.0056 $m^3\ m^{-3}$, respectively with depth. The trend of decreasing values with depth also applied to area density, connectivity, branch number, total branch length and tortuosity, except for pore diameter which did not show apparent variation with depth.

The absolute change in macropore density expressed as a percentage change from the first scanning varied from 50 to 225% for the Transition layer and 86 to 399% for the Compacted layer. In the Compacted layer, this change was significantly different from barley only for chicory and lucerne ($p = 0.019$). While increases in macroporosity varied among the potential subsoilers ($p < 0.05$), they were not significantly larger than barley in any of the studied soil layers, except for tall fescue in the Transition layer. Fig. 3 shows the variation of CT-macroporosity with depth for the crop treatments under study. CT-macroporosity varied markedly with depth down to ~ 0.30 m, whereas little variation occurred between 0.30 and 0.50 m.

Absolute changes in pore area density ranged from 1.1 to 11.9 and from 1.8 to 7.2 $m^2\ m^{-3}$ for the Transition and Compacted layer, respectively, whereas changes in connectivity varied from 0.07 to 1.74 and 0.02 to 0.07 ($\times 10^5$) number m^{-3} (Table 2). In the Compacted layer, increases in area density and connectivity among the potential bio-subsoilers did not differ significantly from barley.

In the Plough layer, the mean weighted pore diameter increased for chicory and radish compared to lucerne and tall fescue ($p = 0.015$), but was not significantly different from that of barley. In both the Transition and Compacted layers, reduction in pore diameter was found

Table 2
X-ray Computed Tomography (CT)-derived pore characteristics for a heavily compacted soil under potential bio-subsoilers. Median values are given for the samples before plant treatment and the absolute change one year after.

Soil layer	Treatment		Macropore density (x10^5) (n_o m^{-3})	Macro-porosity (m^3 m^{-3})	Area density (m^2 m^{-3})	Connectivity (x10^5) (n_o m^{-3})	Mean pore diameter (x10^{-3}) (m)	Branches number	Total branch length (m)	Euclidean tortuosity
Plough	Barley	Before	26.3	0.0543	77.5	2.60	2.38	7267	37.65	1.26
(0.1–0.25 m)		Change	*11.7*	*−0.0016 ab*	*−1.2*	*−0.89*	*−0.03 ab*	*−367*	*1.10*	*0.0004*
	Chicory	Before	33.8	0.0815	101.6	6.12	2.45	9680	52.48	1.26
		Change	*11.7*	*0.0007b*	*−15.3*	*−3.47*	*1.51b*	*−929*	*−11.29*	*−0.0937*
	Lucerne	Before	38.7	0.1044	125.1	8.02	2.67	12,499	68.50	1.26
		Change	*−0.3*	*−0.0322 a*	*−26*	*−4.35*	*−0.20 a*	*−2338*	*−19.98*	*−0.0911*
	Radish	Before	9.9	0.0378	48.7	1.69	2.29	3933	22.49	1.26
		Change	*3.1*	*0.0001b*	*1.8*	*−0.53*	*0.05b*	*60*	*−0.14*	*−0.0126*
	Tall fescue	Before	28.4	0.0956	121.2	5.63	2.73	11,697	60.74	1.26
		Change	*7.4*	*−0.0134 ab*	*−12.2*	*−2.86*	*−0.24 a*	*−2469*	*−10.78*	*−0.0022*
p-value treatment effect for absolute change			0.261	0.045	0.086	0.115	0.015	0.116	0.086	0.087
Transition	Barley	Before	1.9	0.0080	11.5	0.07	2.45	482	3.00	1.22
(0.25–0.35 m)		Change	*3.3*	*0.0039 bc*	*6.1*	*0.25*	*−0.06*	*571*	*3.07*	*0.0032*
	Chicory	Before	1.7	0.0132	17.8	0.16	2.59	652	4.68	1.24
		Change	*4.6*	*0.0054 bc*	*7.5*	*0.29*	*−0.07*	*1255*	*3.79*	*−0.0906*
	Lucerne	Before	8.4	0.0390	50.3	1.74	2.59	2811	15.61	1.26
		Change	*4.0*	*0.0060c*	*11.9*	*0.18*	*−0.15*	*1652*	*4.83*	*−0.0784*
	Radish	Before	0.6	0.0108	11.7	0.16	2.90	458	3.36	1.24
		Change	*1.4*	*0.0033b*	*6.1*	*0.27*	*−0.19*	*370*	*2.10*	*0.0166*
	Tall fescue	Before	5.0	0.0186	24.2	0.38	2.67	1083	6.51	1.25
		Change	*3.0*	*0.0007 a*	*1.1*	*0.02*	*−0.24*	*70*	*0.57*	*−0.0135*
p-value treatment effect for absolute change			0.202	0.037	0.098	0.468	0.754	0.240	0.163	0.240
Compacted	Barley	Before	*0.4*	*0.0031*	*4.5*	*0.03*	*2.49*	*213*	*1.90*	*1.16*
(0.35–0.50 m)		Change	*0.6 a*	*0.0019 ab*	*2.8 ab*	*0.10*	*−0.25*	*244 a*	*1.48 ab*	*0.0136*
	Chicory	Before	0.5	0.0040	5.7	0.02	2.47	254	2.09	1.16
		Change	*2.0b*	*0.0029b*	*4.4b*	*0.09*	*−0.18*	*873b*	*2.80 bc*	*−0.0378*
	Lucerne	Before	0.9	0.0091	12.3	0.07	2.64	450	4.19	1.16
		Change	*2.1b*	*0.0043b*	*7.2b*	*0.29*	*−0.31*	*1418b*	*4.69c*	*−0.0120*
	Radish	Before	0.6	0.0043	6.1	0.04	2.46	293	2.31	1.17
		Change	*0.5 a*	*0.0006 a*	*1.8 a*	*−0.01*	*−0.03*	*100 a*	*0.76 a*	*−0.0015*
	Tall fescue	Before	1.1	0.0072	10.2	0.03	2.57	354	3.76	1.16
		Change	*1.0 ab*	*0.0013 a*	*1.8 a*	*0.02*	*−0.12*	*129 a*	*0.84 a*	*−0.0111*
p-value treatment effect for absolute change			0.019	0.029	0.032	0.060	0.359	0.050	0.027	0.161

Absolute change refers to the simple difference in the parameter over the two periods, i.e. Absolute change = value of the parameter one year after plant treatment – value of the parameter before plant treatment. The non-parametric test, Kruskal–Wallis, was used to test the effects of the potential bio-subsoilers on the absolute change of each CT-derived pore characteristic, considering 5% of significance level.

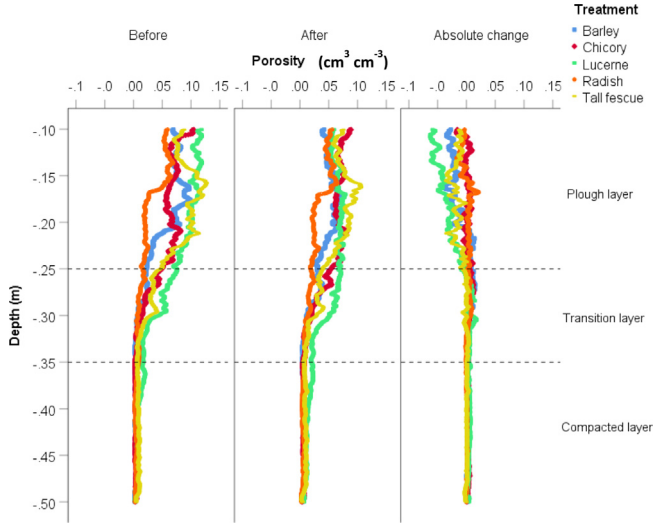

Fig. 3. X-ray Computed Tomography-derived macroporosity distribution for heavily compacted samples Before plant treatment, one year After plant treatment, and the Absolute change in depth. Absolute change refers to the simple difference in the parameter over the two periods, i.e. Absolute change = value of the parameter one year after plant treatment – value of the parameter before plant treatment. Values shown are arithmetic means of three replicates.

for all the treatments, but differences were not significant ($p > 0.10$).

No significant bio-subsoiler effect was found for branch number in the Plough and Transition layer. However, in the Plough layer branch number had a negative absolute change under the plant treatments, except for radish, but a positive absolute change in the Transition layer. Similar to pore density, a significant increase was observed in the number of branches under chicory and lucerne compared to barley ($p = 0.050$) in the Compacted layer.

The absolute change of total branch length decreased after one year in the Plough layer, but increased in the Transition and Compacted layer. Increment in total branch length was significant for lucerne compared to barley, radish and tall fescue ($p = 0.027$) in the Compacted layer.

The absolute change of Euclidean tortuosity was positive for barley but negative for the potential subsoilers in the three layers, although the difference to barley was not significant in any soil layer.

3.2. Pore size distribution

Fig. 4a (Table A) illustrates the absolute change in pore volume as a function of pore size diameter. In the Plough layer, a trend of decreasing in the volume of pores for the size range of 2.5–3 mm for all the treatments, except for radish, was observed. There was a trend of chicory to have a larger change in pore volume for pores > 3 mm in diameter compared to the other treatments in the Plough layer ($p = 0.086$). In the Transition layer, lucerne had a smaller increase in pore volume for pores with a mean diameter of < 1.5 mm compared to

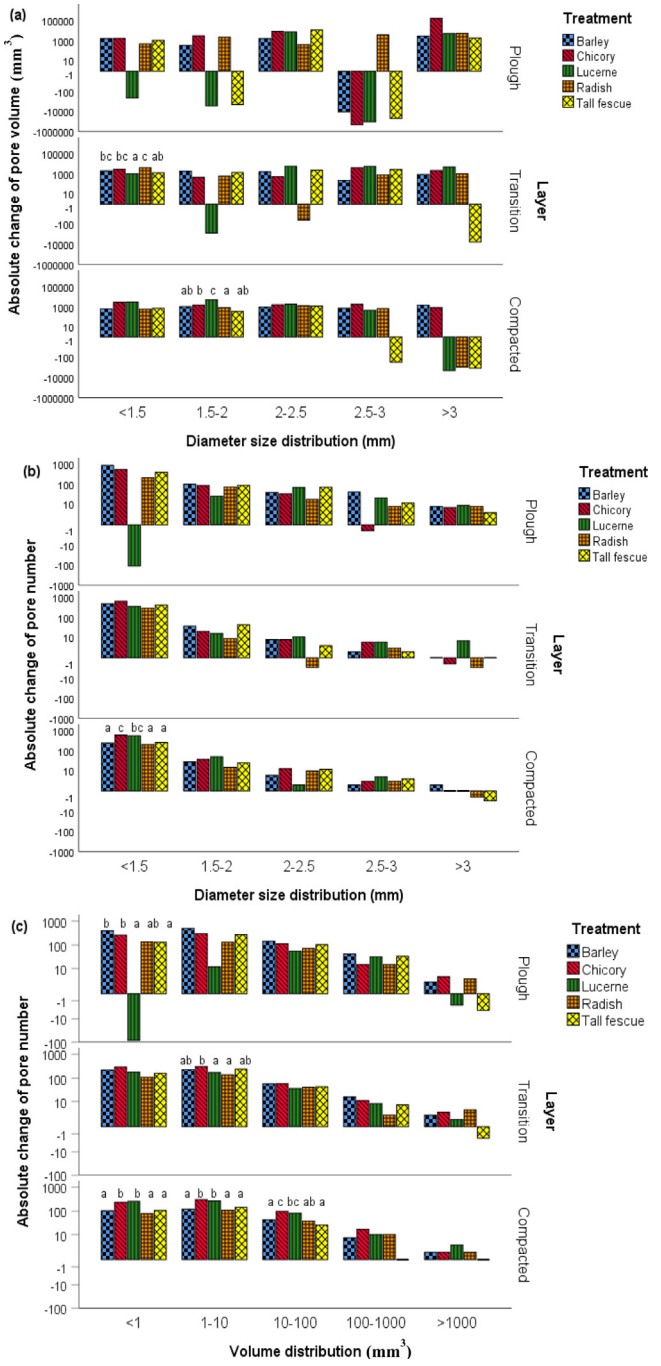

Fig. 4. Distribution of pore volume (a) and pore number (b) as a function of diameter size intervals and the distribution of number of macropores (c) as a function of volume intervals. Pore parameters were quantified using a medical X-ray Computed Tomography scanner. Plough, Transition and Compacted layer depths are 0.10–0.25, 025–0.35 and 0.35–050 m, respectively. Absolute change refers to the simple difference in the parameter over the two periods, i.e. Absolute change = (value of the parameter one year after plant treatment – value of the parameter before plant treatment). The non-parametric test, Kruskal–Wallis, was used to test the effects of the potential biological subsoilers on the absolute change of each size interval, considering 5% of significance level.

barley, chicory and radish ($p = 0.050$). Lucerne reached the most substantial increase in pore volume for pores with a diameter of 1.5–2.0 mm ($p = 0.046$) in the Compacted layer.

When pore number was grouped according to pore size diameter (Fig. 4b, Table A), the biggest changes in the number of pores were observed for pores with diameter < 2 mm in all layers. However, in the Plough layer the change in pore number for the different pore sizes did not significantly vary among crop treatments. In the Transition layer, chicory showed an increasing trend in the number of pores with diameter < 1.5 mm ($p = 0.055$) compared to lucerne, radish and tall fescue. There was, however, no significant difference to barley. There was also a trend that chicory or lucerne show larger change in pore number for pores < 1.5 mm ($p = 0.049$) and 1.5–2 mm ($p = 0.098$) in diameter compared to barley in the Compacted layer.

The results in Fig. 4c (Table B), where the absolute change in pore number is plotted as a function of pore volume intervals, indicate that differences among treatments were only significant ($p \leq 0.05$) at the Transition and Compacted layers. Chicory had the largest absolute change in pore number in the Transition layer for pores 1–10 mm^3 and was significantly larger compared to lucerne and radish, but not significantly different from barley ($p = 0.054$). For the Compacted layer, both chicory and lucerne showed an increase in pore number (relative percentage between ~60–150%) compared to barley for volume sizes of < 1 ($p = 0.050$), 10–100 ($p = 0.035$) and 100–1000 ($p = 0.033$) mm^3. In none of the soil layers did radish and tall fescue differ significantly from barley at the mentioned volume intervals.

3.3. Pore shape classification

In the Plough layer, there were evident trends in pore shape changes (Fig. 5, Table C). After one year under crop treatment, barley showed a decrease in the volume of non-classified pores, however, increased in number and showed no significant change in mean diameter. For chicory, radish and tall fescue, trends of increases in pore volume, number and diameter were displayed for non-classified pores. For these three crops there was a large reduction in pore volume with an increase in quantity for oblate pores. Whereas for lucerne, oblate and tri-axial pores decreased in volume, number and diameter.

Non-classified pores dominated the increases in pore volume and number in the Transition layer for all the crop treatments. Oblate and tri-axial pores, however, showed general trend of a reduction in pore volume and diameter for the potential subsoilers. At the Transition layer equant and prolate pores increased in diameter for lucerne, but this was limited to prolate under tall fescue. The volume and number of prolate pores increased in all the layers in all the crop treatments.

For the Compacted layer, there was a clear trend of a larger increase in pore number of non-classified pores for the chicory and lucerne treatment, but in terms of pore volume this did not seem to differ widely from the other plant treatments. Oblate pores for radish and tall fescue, but also tri-axial for tall fescue, showed a lower contribution to pore volume but increase in number after one year. In this dense layer, the largest reduction in pore diameter of non-classified pores was for soil under barley. Chicory and lucerne showed a decrease in diameter for all pore shapes, except equant, which increased slightly after one year of the experiment.

4. Discussion

4.1. Effect of potential bio-subsoilers on pore network

A decline in pore network density with depth was visualised and quantified using the CT images of the samples before the establishment of the experiment. The variation of CT-macroporosity with depth in Fig. 3 supports the partitioning of the soil columns into three representative layers of the structural difference with depth, e.g., loose structure (0.1–0.25 m), transitioning state (0.25–0.35 m) and dense structure (0.35–0.50 m). Although the CT-macroporosity distribution with depth was very similar for all the crop treatments, the second scan event revealed changes in pore network that differed among plant treatments and attributed to root development.

In the Plough layer changes in pore network (decrease in CT-

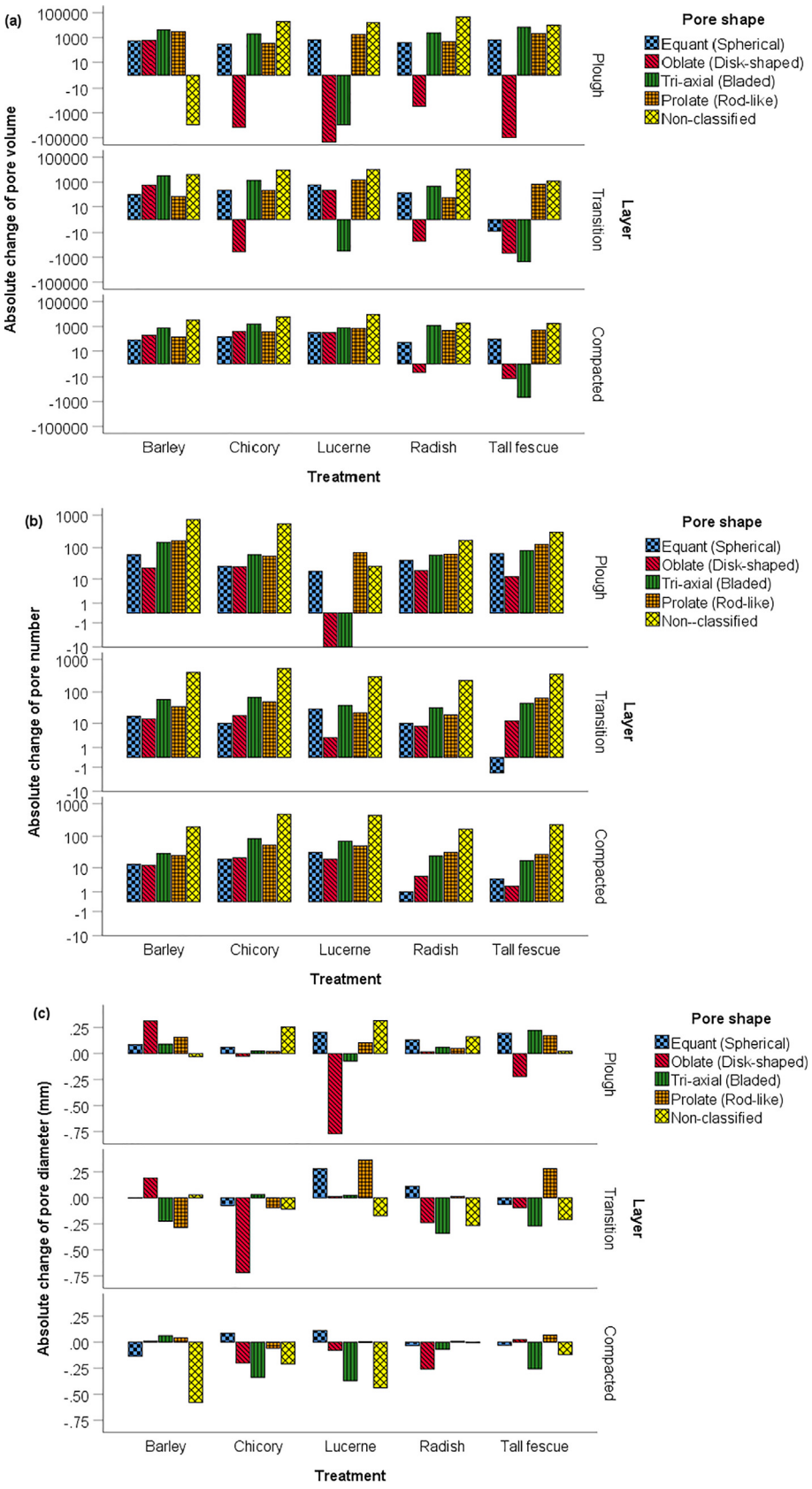

Fig. 5. Distribution of the absolute change of macropore volume (a), number (b) and diameter (c) as a function of pore shape. Pore parameters were quantified using a medical X-ray Computed Tomography scanner. Plough, Transition and Compacted layer depths are 0.10–0.25, 025–0.35 and 0.35–050 m, respectively. Absolute change refers to the simple difference in the parameter over the two periods, i.e. Absolute change = value of the parameter one year after plant treatment – value of the parameter before plant treatment.

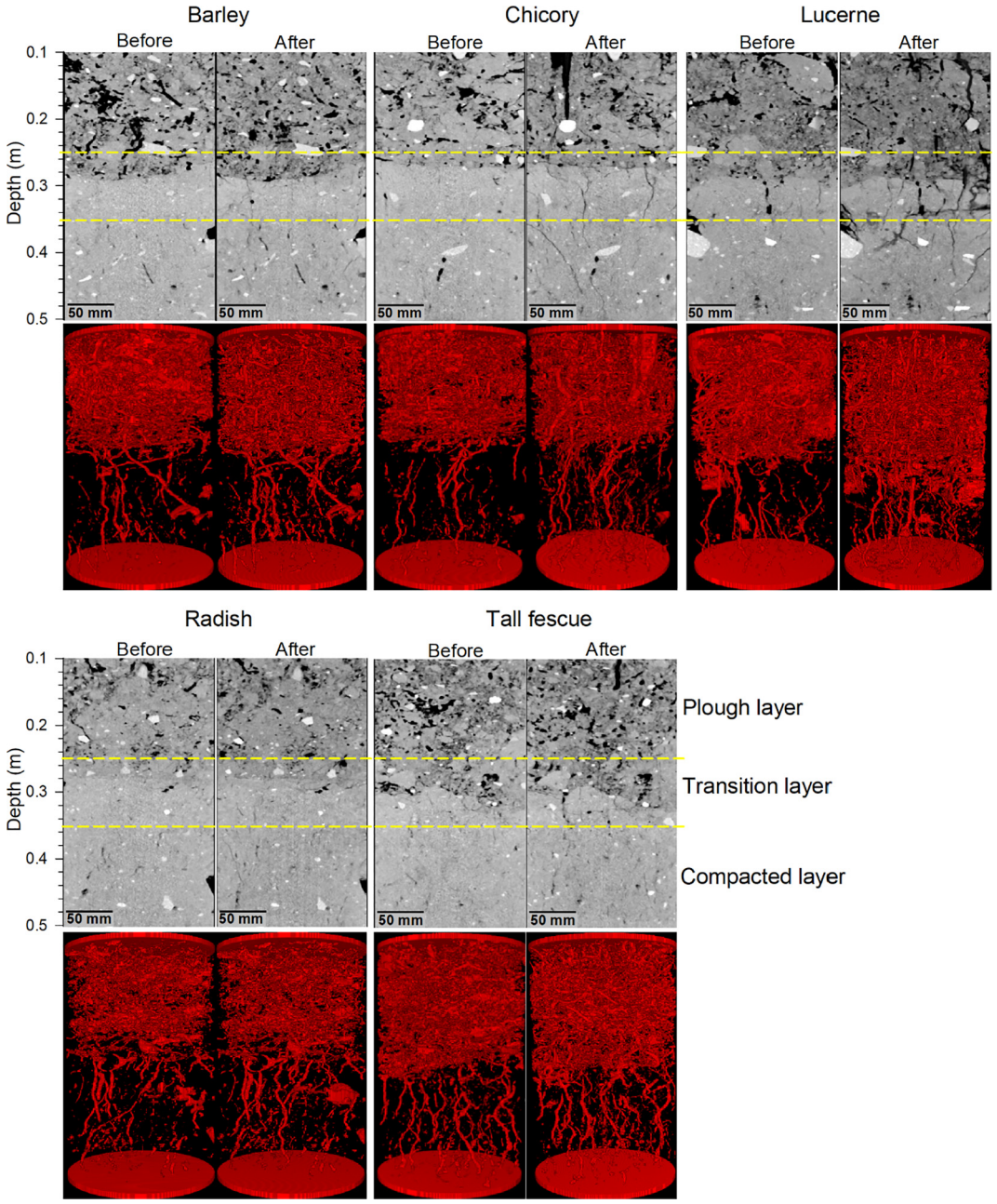

Fig. 6. Grey images of vertical cross-sections for representative samples from each plant treatment, before and after 1 year under potential bio-subsoilers. Below each grey images are the respective 3-D renderings of the pores analysed in this study.

macroporosity, area density, connectivity and branch length) are related to soil consolidation by settling, wetting and drying cycles and root growth compression (Koestel and Schlüter, 2019). Beneath this top layer, changes are expected to result from the roots attempting to penetrate the hard layer (Lamandé et al., 2013). Our results (Fig. 4) show evidence of several pores of small volume and diameter in the Transition layer and especially in the Compacted layer, which is an important initial state in the mitigation of compaction. It is worth noting that the average pore diameters were reduced for all the treatments in both the Transition and Compacted layers (Table 2). This can be attributed to the increase in the density of small pores, i.e., pores with small diameter and volume resulting in a reduction in the mean pore diameter, which in turn may be associated with the development of fine roots during one year.

Interestingly, the vertical cross-section (Fig. 6) displayed soil cracking and an apparent increase in macropore volume in the Transition layer (0.25–0.35 m depth) after the plant growing. Positive effects of cover crops in the transition between the top and the hard layer have been reported by previous studies (Abdollahi et al., 2014). In the Compacted layer (0.35–0.50 m), the pore number under chicory and lucerne was, respectively, 110 and 81% higher than the initial pore number. This represents 2.1 and 1.6 times the increase found for barley. The significant increase in CT- macropore density, branch number and total branch length produced by chicory and lucerne in the Compacted layer implies the development of a larger, more connected and complex pore network than the pre-existing one. According to Munkholm et al. (2012), this implies an increased likelihood of crack propagation and interaction in the soil if stressed in tension mode. In the Compacted layer, cracks, fissures or biopores are visible in the vertical cross-sections of representative samples (Fig. 6), especially for soil columns under chicory and lucerne.

Radish and tall fescue did not show a statistically significant trend

for increasing pore network density. However, a few visible cracks were formed one year after the initiation of the experiment (Fig. 6), which can also be attributed to root pressure or to wetting and drying.

Regarding connectivity, there was no significant effect of the potential bio-subsoilers. Results from Pires et al. (2017) suggest that high connectivity is related to the larger contribution of macropores > 1000 mm^3 to CT-macroporosity. The relatively large increase in number and volume of small disconnected pores compared to the large pores in all the treatments was observed. This suggests that the effectiveness of different bio-subsoilers in altering more complex properties related to soil structure such as connectivity of macropores are not clear within a year of crop growth. Possibly, most of the effect of the bio-subsoilers are occurring for pores smaller than those resolved and quantified in this study.

In this study, changes in tortuosity with depth and among plant treatments were negligible. For the Compacted layer, this may be explained by an incipient root system after one year of growing the different crops. As illustrated by Hu et al. (2015), high porosity and tortuosity may be associated with well-developed root systems. However, it is worth noting that our results refer to an average value for tortuosity of large CT-pores, and which is influenced by small pores that are usually large in number but have very low tortuosity values (close to 1). Pires et al. (2017) suggest that increases in tortuosity with depth and number of pores favour the formation of pores of irregular shape. In the present study, non-classified pores had the highest increase in number after one year of the experiment. This indicates an increase in complexity of the pore networks with more interconnected pores. For chicory and lucerne it is worth noting that 3D tri-axial and prolate pore shapes also contributed to the number of pores created, which tended to constitute a larger proportion than for barley and other plant treatments. According to Luo et al. (2010), macropores formed by roots are highly continuous, round in shape, and decrease in size with depth.

The 3D renderings of the pores analysed from the whole soil columns shown in Fig. 6 reveal elongated and continuous, large macropores that are visible in the Compacted layer before crop treatment. These macropores could be biopores that are not affected by traffic stress (Schäffer et al., 2008) and that are maintained by earthworms or persist after the decay of former large roots (Kautz, 2015). They may also have been formed after compaction, as earthworm burrowing is possible in dense soils if not too dry (Whalley et al., 1995). As mentioned previously, one year after initiation of the experiment, the number of pores in the Compacted layer was mainly dominated by pores < 100 mm^3 (Fig. 4c). Additionally, a few pores > 1000 mm^3 with diameter > 2.5 mm were formed (ranging from two to four in the plant treatments), which most probably represent new earthworm burrows (Luo et al., 2010).

In Fig. 6, the 3D images of the soil columns show small, randomly distributed and less continuously distributed macropores after plant growth. The formation of new biopores and the related cracks in hard layers would likely enhance pore connectivity with time, which consequently improves root exploration even in soils with dense, hard layers, especially in drier years (Galdos et al., 2019).

4.2. Role of plant/root type in compaction mitigation

The studied potential bio-subsoilers differed in their impact on the soil pore characteristics in the Compacted subsoil layer. The most common taproot cover crops assessed as potential bio-subsoilers are the brassicas (e.g., Chen and Weil, 2010; Abdollahi et al., 2014; Gruver et al., 2014; Guaman et al., 2016). Chen and Weil (2010) showed that fodder radish had greater penetration capability and root number than rye and rapeseed on compacted, fine loamy soils. The authors attributed the root penetration capacity of fodder radish through hard layers to its root architecture, i.e., a single, dominant, cylindrically-shaped, fleshy taproot with thick branch roots and dense fine rooting with depth. Abdollahi and Munkholm (2014) found that five consecutive years of forage radish on a sandy loam soil favoured mitigation of soil compaction (decreased penetration resistance) at 0.3–0.6 m depth.

However, in our study radish did not show a significantly different impact on the pore network compared with the reference barley for severely compacted subsoil. This is in agreement with Guamán Sarango (2015) who found no apparent mitigation effect of fodder radish in compacted soil with 3 MPa of penetration resistance at 0.3–0.6 m depth. The authors hypothesised that the full potential of the crop was not realised due to the short growing period of two years.

Our results show that for the CT-pore parameters quantified, tall fescue had a similar effect to radish and barley on the CT-porosity of the Compacted layer. Conversely, the root systems of chicory and lucerne positively affected CT- porosity at 0.3–0.5 m depth.

A root characterisation study conducted by Gentile et al. (2003) of, respectively, 2, 3 and 11 years of growing tall fescue, chicory and lucerne in a silty clay loam soil showed that tall fescue and chicory had a large number of root axes and root biomass at 0.2–0.3 m depth whereas lucerne had a greater number of root axes and root branching at 0.2–0.6 m depth. Tall fescue is characterised, like most grasses, by having a fibrous root system with a very small diameter that remains relatively constant with soil depth, while lucerne and chicory are taproot crops with larger root diameter that varies with depth (Gentile et al., 2003; Han et al., 2015). The root diameter was given by Perkons et al. (2014) as the reason for the greater number of large-sized biopores per unit surface area up to 0.65 m depth after chicory compared to tall fescue in a Luvisol in Germany.

Even though root characterisation was not the scope of our study, the differences in terms of root density, root branching and root diameter among the cover crops under study would appear to explain the dissimilarities in how they function as bio-subsoilers. It is worth noting that crop density could also play an essential role in the results obtained. For instance, lucerne with its higher crop density resulted in a larger number of biopores than chicory in a Luvisol in Germany (Han et al., 2015). In our study, the ranking in decreasing order of crop density was lucerne > tall fescue > barley > chicory > radish. It is important to note that radish is an annual crop with a fine root diameter at depth and low crop density, while the perennial crops such us chicory and lucerne can develop more extensive root systems over time (Gentile et al., 2003), which is expected to provide a greater potential as bio-subsoiler in the subsoil.

The fact that the root system of chicory and lucerne showed a greater ability to impact soil macroporosity in the Compacted layer after only one year as a cover crop it is of high importance. Although CT-derived macroporosity (> 0.86 mm in diameter) was < 0.05 m^3 m^{-3} in the Compacted layer, chicory and lucerne increased CT-derived macroporosity by, respectively, 94 and 52% in relation to the initial porosity at the start of the experiment. Small increases in pore volume beyond a minimum rooting density had a strong effect on soil porosity (Bodner et al., 2014), which in time is anticipated to be of high importance in subsoil compaction mitigation.

5. Conclusion

CT-geometrical soil pore characteristics tested in this study differed for the five bio-subsoilers after one year of the experiment. In the Compacted layer, at 0.35–0.50 m depth, chicory and lucerne had a significant positive impact on porosity (> 0.86 mm in diameter). Therefore, they can be expected to perform better than radish and tall fescue when used as a bio-subsoilers for compaction mitigation under the studied conditions. In all cases, the Compacted layer showed small changes in pore system, suggesting that it was still very compact after one year of growing the different crops. We suggest longer-term studies of plant-induced mitigation of compacted subsoils involving different soil types and climate conditions. The changes in pore network found in this study are relevant, since even small increases in macroporosity and changes in pore network can potentially boost the dynamics or

mitigation processes in deep compacted subsoils that take place over time.

Acknowledgements

The assistance during sample collection and establishment of the experiment of Stig T. Rasmussen, Michael Koppelgaard, Jens Bonderup Kjeldsen and Kim Møller Johansen from Aarhus University, Denmark, is gratefully acknowledged. The authors also thank Søren Baarsgaard Hansen at the PET-Center, Aarhus University Hospital, Denmark, for the technical support in scanning the soil samples. This work was funded by the Ministry of Environment and Food of Denmark via the COMMIT project (GUDP Grant 571 no. 34009-16-1086). We are also thankful to the anonymous referees for their helpful comments and suggestions.

Appendix A. Supplementary data

Supplementary data to this article can be found online at https://doi.org/10.1016/j.geoderma.2019.114154.

References

Abdollahi, L., Munkholm, J., Garbout, A., 2014. Tillage system and cover crop effects on soil quality: II. Pore characteristics. Soil Sci. Soc. Am. J 78, 271–279.
Abdollahi, L., Munkholm, L.J., 2014. Tillage system and cover crop effects on soil quality: I. Chemical, mechanical, and biological properties. Soil Sci. Soc. Am. J. 78, 262–270.
Abràmoff, M.D., Magalhães, P.J., Ram, S.J., 2004. Image processing with Image. J. Biophotonics Int. 11, 36–42.
Arvidsson, J., 2001. Subsoil compaction caused by heavy sugarbeet harvesters in southern Sweden: I. Soil physical properties and crop yield in six field experiments. Soil Tillage Res. 60, 67–78.
Arvidsson, J., Håkansson, I., 2014. Response of different crops to soil compaction—Short-term effects in Swedish field experiments. Soil Tillage Res. 138, 56–63.
Berisso, F.E., Schjønning, P., Keller, T., Lamandé, M., Simojoki, A., Iversen, B.V., Alakukku, L., Forkman, J., 2013. Gas transport and subsoil pore characteristics: anisotropy and long-term effects of compaction. Geoderma 195, 184–191.
Bodner, G., Leitner, D., Kaul, H.-P., 2014. Coarse and fine root plants affect pore size distributions differently. Plant Soil 380, 133–151.
Bullock, P., Fedoroff, N., Jongerius, A., Stoops, G., Tursina, T., 1985. Handbook for soil thin section description. Waine Research.
Carminati, A., Vetterlein, D., Weller, U., Vogel, H.-J., Oswald, S.E., 2009. When roots lose contact. Vadose Zone J. 8, 805–809.
Celette, F., Gaudin, R., Gary, C., 2008. Spatial and temporal changes to the water regime of a Mediterranean vineyard due to the adoption of cover cropping. Eur. J. Agron. 29, 153–162.
Chen, G., Weil, R.R., 2010. Penetration of cover crop roots through compacted soils. Plant Soil 331, 31–43.
Chen, G., Weil, R.R., 2011. Root growth and yield of maize as affected by soil compaction and cover crops. Soil Tillage Res. 117, 17–27.
Chen, G., Weil, R.R., Hill, R.L., 2014. Effects of compaction and cover crops on soil least limiting water range and air permeability. Soil Tillage Res. 136, 61–69.
Clark, L.J., Barraclough, P.B., 1999. Do dicotyledons generate greater maximum axial root growth pressures than monocotyledons? J. Exp. Bot. 50, 1263–1266.
Cooper, J., 2011. The untilt stack plugin for ImageJ.
Cresswell, H., Kirkegaard, J., 1995. Subsoil amelioration by plant-roots-the process and the evidence. Soil Res. 33, 221–239.
Doube, M., Kłosowski, M.M., Arganda-Carreras, I., Cordelières, F.P., Dougherty, R.P., Jackson, J.S., Schmid, B., Hutchinson, J.R., Shefelbine, S.J., 2010. BoneJ: free and extensible bone image analysis in ImageJ. Bone 47, 1076–1079.
Etana, A., Larsbo, M., Keller, T., Arvidsson, J., Schjønning, P., Forkman, J., Jarvis, N., 2013. Persistent subsoil compaction and its effects on preferential flow patterns in a loamy till soil. Geoderma 192, 430–436.
Galdos, M., Pires, L., Cooper, H., Calonego, J., Rosolem, C., Mooney, S., 2019. Assessing the long-term effects of zero-tillage on the macroporosity of Brazilian soils using X-ray Computed Tomography. Geoderma 337, 1126–1135.
Gentile, R., Martino, D., Entz, M., 2003. Root characterization of three forage species grown in southwestern Uruguay. Can. J. Plant Sci. 83, 785–788.
Głąb, T., 2007. Application of image analysis for soil macropore characterization according to pore diameter. Int. Agrophysics 21, 61–66.
Gruver, J., Weil, R., White, C., Lawley, Y., 2014. Radishes: a new cover crop for organic farming systems. Michigan State University. Retrieved, 10-01.
Guamán Sarango, V., 2015. Biological and mechanical subsoiling in potato production–a participatory research approach. Swedish University of Agricultural Sciences, Uppsala.
Guaman, V., Båth, B., Hagman, J., Gunnarsson, A., Persson, P., 2016. Short time effects of biological and inter-row subsoiling on yield of potatoes grown on a loamy sand, and on soil penetration resistance, root growth and nitrogen uptake. Eur. J. Agron. 80, 55–65.
Han, E., Kautz, T., Perkons, U., Lüsebrink, M., Pude, R., Köpke, U., 2015. Quantification of soil biopore density after perennial fodder cropping. Plant Soil 394, 73–85.
Hu, X., Li, Z.-C., Li, X.-Y., Liu, Y., 2015. Influence of shrub encroachment on CT-measured soil macropore characteristics in the Inner Mongolia grassland of northern China. Soil Tillage Res. 150, 1–9.
Hubbard, R.K., Strickland, T.C., Phatak, S., 2013. Effects of cover crop systems on soil physical properties and carbon/nitrogen relationships in the coastal plain of southeastern USA. Soil Tillage Res. 126, 276–283.
Jones, R.J., Spoor, G., Thomasson, A., 2003. Vulnerability of subsoils in Europe to compaction: a preliminary analysis. Soil Tillage Res. 73, 131–143.
Katuwal, S., Arthur, E., Tuller, M., Moldrup, P., de Jonge, L.W., 2015a. Quantification of soil pore network complexity with X-ray computed tomography and gas transport measurements. Soil Sci. Soc. Am. J. 79, 1577–1589.
Katuwal, S., Moldrup, P., Lamandé, M., Tuller, M., De Jonge, L.W., 2015b. Effects of CT number derived matrix density on preferential flow and transport in a macroporous agricultural soil. Vadose Zone J. 14.
Katuwal, S., Norgaard, T., Moldrup, P., Lamandé, M., Wildenschild, D., de Jonge, L.W., 2015c. Linking air and water transport in intact soils to macropore characteristics inferred from X-ray computed tomography. Geoderma 237, 9–20.
Kautz, T., 2015. Research on subsoil biopores and their functions in organically managed soils: a review. Renew. Agric. Food Syst. 30, 318–327.
Keller, T., Colombi, T., Ruiz, S., Manalili, M.P., Rek, J., Stadelmann, V., Wunderli, H., Breitenstein, D., Reiser, R., Oberholzer, H., 2017. Long-term soil structure observatory for monitoring post-compaction evolution of soil structure. Vadose Zone J. 16, 1–16.
Koestel, J., Schlüter, S., 2019. Quantification of the structure evolution in a garden soil over the course of two years. Geoderma 338, 597–609.
Lamandé, M., Wildenschild, D., Berisso, F.E., Garbout, A., Marsh, M., Moldrup, P., Keller, T., Hansen, S.B., de Jonge, L.W., Schjønning, P., 2013. X-ray CT and laboratory measurements on glacial till subsoil cores: Assessment of inherent and compaction-affected soil structure characteristics. Soil Sci. 178, 359–368.
Legland, D., Arganda-Carreras, I., Andrey, P., 2016. MorphoLibJ: integrated library and plugins for mathematical morphology with ImageJ. Bioinformatics 32, 3532–3534.
Lipiec, J., Hatano, R., 2003. Quantification of compaction effects on soil physical properties and crop growth. Geoderma 116, 107–136.
Löfkvist, J., 2005. Modifying soil structure using plant roots. Swedish University of Agricultural Sciences, Uppsala.
Luo, L., Lin, H., Li, S., 2010. Quantification of 3-D soil macropore networks in different soil types and land uses using computed tomography. J. Hydrol. 393, 53–64.
Lynch, J.P., Wojciechowski, T., 2015. Opportunities and challenges in the subsoil: pathways to deeper rooted crops. J. Exp. Bot. 66, 2199–2210.
Materechera, S., Alston, A., Kirby, J., Dexter, A., 1992. Influence of root diameter on the penetration of seminal roots into a compacted subsoil. Plant Soil 144, 297–303.
Materechera, S., Dexter, A., Alston, A.M., 1991. Penetration of very strong soils by seedling roots of different plant species. Plant Soil 135, 31–41.
Munkholm, L.J., Heck, R.J., Deen, B., 2012. Soil pore characteristics assessed from X-ray micro-CT derived images and correlations to soil friability. Geoderma 181, 22–29.
Munkholm, L.J., Schjønning, P., Jørgensen, M.H., Thorup-Kristensen, K., 2005. Mitigation of subsoil recompaction by light traffic and on-land ploughing: II. Root and yield response. Soil Tillage Res. 80, 159–170.
Naveed, M., Moldrup, P., Arthur, E., Wildenschild, D., Eden, M., Lamandé, M., Vogel, H.-J., De Jonge, L.W., 2013. Revealing soil structure and functional macroporosity along a clay gradient using X-ray computed tomography. Soil Sci. Soc. Am. J. 77, 403–411.
Naveed, M., Schjønning, P., Keller, T., de Jonge, L.W., Moldrup, P., Lamandé, M., 2016. Quantifying vertical stress transmission and compaction-induced soil structure using sensor mat and X-ray computed tomography. Soil Tillage Res. 158, 110–122.
Perkons, U., Kautz, T., Uteau, D., Peth, S., Geier, V., Thomas, K., Holz, K.L., Athmann, M., Pude, R., Köpke, U., 2014. Root-length densities of various annual crops following crops with contrasting root systems. Soil Tillage Res. 137, 50–57.
Pfeifer, J., Kirchgessner, N., Colombi, T., Walter, A., 2015. Rapid phenotyping of crop root systems in undisturbed field soils using X-ray computed tomography. Plant Meth. 11, 41.
Phansalkar, N., More, S., Sabale, A., Joshi, M., 2011. Adaptive local thresholding for detection of nuclei in diversity stained cytology images. In: 2011 International Conference on Communications and Signal Processing (ICCSP). IEEE, pp. 218–220.
Pires, L., Roque, W., Rosa, J., Mooney, S., 2019. 3D analysis of the soil porous architecture under long term contrasting management systems by X-ray computed tomography. Soil Tillage Res. 191, 197–206.
Pires, L.F., Borges, J.A., Rosa, J.A., Cooper, M., Heck, R.J., Passoni, S., Roque, W.L., 2017. Soil structure changes induced by tillage systems. Soil Tillage Res. 165, 66–79.
Pulido-Moncada, M., Munkholm, L.J., Schjønning, P., 2019. Wheel load, repeated wheeling, and traction effects on subsoil compaction in northern Europe. Soil Tillage Res. 186, 300–309.
Raper, R., Reeves, D., Burmester, C., Schwab, E., 2000. Tillage depth, tillage timing, and cover crop effects on cotton yield, soil strength, and tillage energy requirements. Appl. Eng. Agric. 16, 379–386.
Schäffer, B., Mueller, T.L., Stauber, M., Müller, R., Keller, M., Schulin, R., 2008. Soil and macro-pores under uniaxial compression. II. Morphometric analysis of macro-pore stability in undisturbed and repacked soil. Geoderma 146, 175–182.
Schjønning, P., Lamandé, M., Munkholm, L.J., Lyngvig, H.S., Nielsen, J.A., 2016. Soil precompression stress, penetration resistance and crop yields in relation to differently-trafficked, temperate-region sandy loam soils. Soil Tillage Res. 163, 298–308.
Snapp, S., Swinton, S., Labarta, R., Mutch, D., Black, J., Leep, R., Nyiraneza, J., O'neil, K., 2005. Evaluating cover crops for benefits, costs and performance within cropping system niches. Agron. J. 97, 322–332.
Vogel, H.-J., Weller, U., Schlüter, S., 2010. Quantification of soil structure based on

Minkowski functions. Comput. Geosci. 36, 1236–1245.
Weil, R., Kremen, A., 2007. Thinking across and beyond disciplines to make cover crops pay. J. Sci. Food Agric. 87, 551–557.
Whalley, W., Dumitru, E., Dexter, A., 1995. Biological effects of soil compaction. Soil Tillage Res. 35, 53–68.
Williams, S.M., Weil, R.R., 2004. Crop cover root channels may alleviate soil compaction effects on soybean crop. Soil Sci. Soc. Am. J. 68, 1403–1409.
Zappala, S., Mairhofer, S., Tracy, S., Sturrock, C.J., Bennett, M., Pridmore, T., Mooney, S.J., 2013. Quantifying the effect of soil moisture content on segmenting root system architecture in X-ray computed tomography images. Plant Soil 370, 35–45.